Astron. Astrophys. 342, L53–L56 (1999)

ASTRONOMY AND ASTROPHYSICS

LETTER

Letter to the Editor

Modal tomography for adaptive optics

Roberto Ragazzoni[1], **Enrico Marchetti**[2], **and François Rigaut**[3]

[1] Astronomical Observatory of Padova, vicolo dell'Osservatorio 5, I-35122 Padova, Italy
[2] Centro Galileo Galilei, Apartado 565, E-38700 Santa Cruz de La Palma, Spain
[3] Southern European Observatory, Karl Schwarzschild Strasse 2, D-85386 Garching bei München, Germany

Received 26 October 1998 / Accepted 17 January 1999

Abstract. Multiple Laser Guide Stars can be used to retrieve the three–dimensional distribution of the perturbing layers on the coming wavefront in Adaptive Optics system and to derive corrections for conical anisoplanatism. We outline the basic analytical details of a modal approach to this problem. The advantages of this approach with respect to the traditional zonal one are pointed out along with a preliminary discussion of the way the involved matrices are to be treated in order to minimize noise propagation problems.

Key words: instrumentation: adaptive optics – atmospheric effects – telescopes

1. Introduction

Laser Guide Stars (LGSs) as reference beacon for Adaptive Optics (AO) compensation (Foy & Labeyrie, 1985; Happer et al., 1994) potentially provide diffraction–limited imaging capabilities over the whole sky for large ground based telescopes. Focal anisoplanatism (Fried & Belsher, 1994; Parenti & Sasiela, 1994) is (along with absolute tip–tilt retrieval, not addressed here) a fundamental limitation of LGS adaptive optics.

Several schemes to correct for focal anisoplanatism have been proposed (Sasiela, 1994; Fried, 1995). Three-dimensional tomography (Tallon & Foy 1990, TF90 hereafter) sounds like one of the most promising technique to fully correct focal anisoplanatism.

Based on the same tomography concept, we propose here a *modal* approach to the 3D–sensing, in contrast with the *zonal* approach proposed in TF90. There are several potential advantages of the modal approach. In TF90 layers are subdivided into a grid and rays are geometrically traced from the pupil to LGSs and science object. Noise can be introduced when rays passing within a given grid position are considered as characterizing the whole grid portion (on the other hand, interpolation introduces even further arithmetic manipulation problems) while the modal approach does not imply any of these assumption. In addition, the modal approach allows naturally modal filtering and can be easily extended to non–circular (e.g. with central obstruction) pupils.

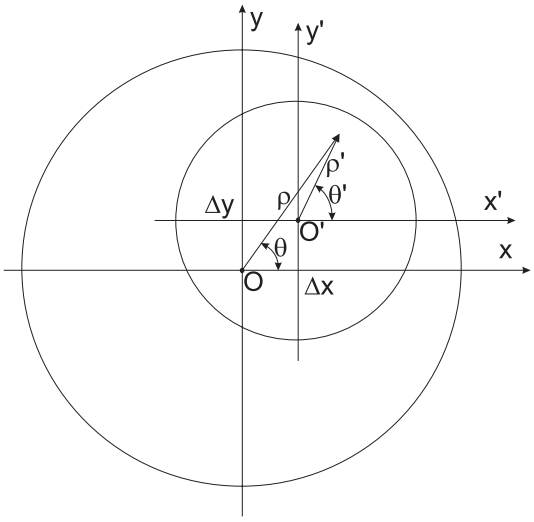

Fig. 1. Definition of the coordinate systems (see text).

2. Zernike polynomials in a circular portion of a pupil

In this section we demonstrate some properties of Zernike polynomials that will be useful in the next section. In the coordinate framework Oxy the usual polar coordinates are defined such that $\rho = 1$ at the edge of the circular pupil centered in O (see Fig. 1). In this framework the wavefront is defined as the sum of Zernike polynomials up to a given radial order Q. This ensemble can always be re–arranged in terms of Hamilton polynomials as:

$$W(\rho,\theta) = \sum_{n,m=0}^{Q} \rho^n \left[A_{nm}\cos(m\theta) + B_{nm}\sin(m\theta)\right] \qquad (1)$$

where $n \geq m$ and $n - m$ is even. In the case of $m = 0$ clearly the coefficient B_{n0} is meaningless so the total amount of independent coefficents A_{nm} and B_{nm} is given by:

$$\frac{(Q+1)^2 + (Q+1)}{2} = \frac{Q^2 + 3Q + 2}{2} \qquad (2)$$

A smaller circular region inside the original one will be characterized by a coordinate system $O'x'y'$. Such coordinate

system has the origin displaced by Δx and Δy in the Oxy coordinates, and the unit length is k times smaller, where k is the ratio of radii of the smaller vs. the larger circular regions. We demonstrate now that it exists a set A'_{nm}, B'_{nm}, limited by the same highest radial term Q, defined in this region such that the wavefront W' defined within such area match exactly the related portion defined by Eq. (1).

In order to provide such demonstration we recall the François Viète formulae for the cosinus:

$$\begin{aligned}\cos(m\theta) \; &= \cos^m\theta - \tfrac{m(m-1)}{1\cdot 2}\cos^{m-2}\theta\sin^2\theta + \\ &+ \tfrac{m(m-1)(m-2)(m-3)}{1\cdot 2\cdot 3\cdot 4}\cos^{m-4}\theta\sin^4\theta - \ldots\end{aligned} \tag{3}$$

and for the sinus:

$$\begin{aligned}\sin(m\theta) \; &= m\cos^{m-1}\theta\sin\theta - \\ &- \tfrac{m(m-1)(m-2)}{1\cdot 2\cdot 3}\cos^{m-3}\theta\sin^3\theta + \ldots\end{aligned} \tag{4}$$

Using Eqs. (3) and (4) one can write the cosinus term in rectangular coordinates instead of the polar ones, obtaining:

$$\begin{aligned}\cos(m\theta) \; &= \left(x^2+y^2\right)^{-m/2} \times \\ &\times \left[a_{0m}y^m - a_{1m}y^{m-2}x^2 + a_{2m}y^{m-4}x^4 - \ldots\right]\end{aligned} \tag{5}$$

and for the sinus:

$$\begin{aligned}\sin(m\theta) &= \left(x^2+y^2\right)^{-m/2} \times \\ &\times \left[b_{0m}y^{m-1}x - b_{1m}y^{m-3}x^3 + b_{2m}y^{m-5}x^5 - \ldots\right]\end{aligned} \tag{6}$$

Finally Eq. (1) can be rewritten in solely rectangular coordinates as:

$$\begin{aligned}W(x,y) \; &= \sum_{n,m=0}^{Q}\Big\{\left(x^2+y^2\right)^{\frac{n-m}{2}} \times \\ &\times \left[A_{nm}\left(a_{0m}y^m - a_{1m}y^{m-2}x^2 + \ldots\right) + \right. \\ &\left. + B_{nm}\left(b_{0m}y^{m-1}x - b_{1m}y^{m-3}x^3 + \ldots\right)\right]\Big\}\end{aligned} \tag{7}$$

This represent a polynomial in x, y of order Q, here denoted by $P^{(Q)}(x,y)$. The number of independent coefficients of type $x^p y^q$ (obeying to the rule $p+q \le Q$) is the same as described by Eq. (2) so that any $P^{(Q)}(x,y)$ can be described by a proper choice of coefficients of Zernike polynomials up to the Q^{th} radial order. In the case of the smaller circular portion one can write:

$$W'(x',y') = W(\Delta x + kx', \Delta y + ky') = P'^{(Q)}(x,y) \tag{8}$$

with $(n-m)/2$ being an integer greater or equal to zero. This prove the statement at the beginning of this section. In other words, provided a Q–limited Zernike description of a wavefront on a large pupil, any circular portion inside it can be described by another Zernike ensemble, limited to the same Q.

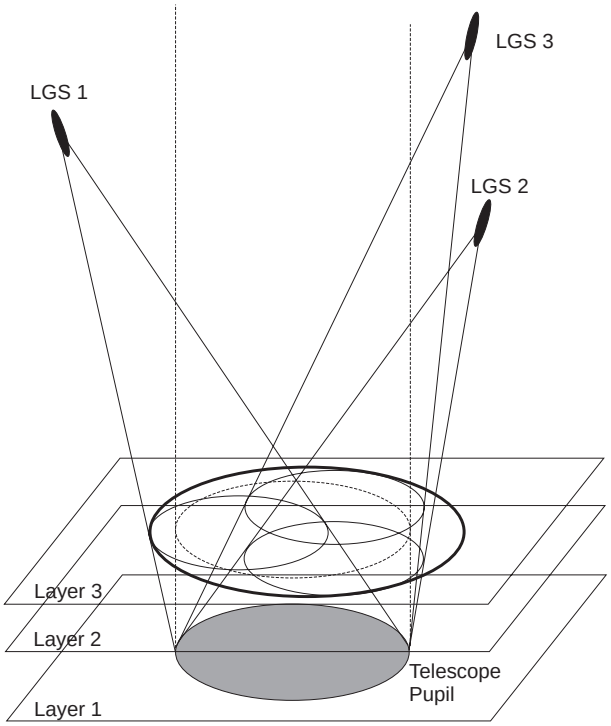

Fig. 2. Geometrical view of the LGSs beam as passes through the perturbing layers and reaches the entrance pupil of the telescope. In this case $N = M = 3$.

3. Modal tomography: Presentation and discussion

We assume in the following that N different LGSs are conveniently projected on the sky and the wavefronts relative to each star are sensed through the telescope entrance pupil by N different wavefront sensors. We also assume that the coming wavefront is perturbed essentially by M layers, located at different altitudes. The geometry of the LGSs, the layers and conical shaped beams down to the telescope is shown in Fig. 2.

In the following we use $i = 1 \ldots N$ as the running index for the LGSs and $j = 1 \ldots M$ as the running index for the perturbing layers.

For the generic j–th layer one can define $N+2$ overlapping regions located on the layer itself. These are the N footprints of the LGSs beam, the footprint of the science object beam down to the telescope and a dummy outer circular region, referred in the following as *metapupil*, encompassing all of the LGSs beams (see Fig. 3).

It is assumed that some circular symmetry is adopted in the relative positions of the LGSs with respect to the telescope pupil and that the science target is aligned with the optical axes of the telescope. These assumptions are essentially similar to the TF90 ones.

The fired LGSs are not *fixed* in the sky because of the upward wandering of the laser beam. This translates into some uncertainty of the exact position of the N footprint on each layer, the error being larger for the highest layers and nulling at the telescope pupil. This error has been discussed in Ragazzoni, Esposito & Riccardi (1998) where it has been shown that under

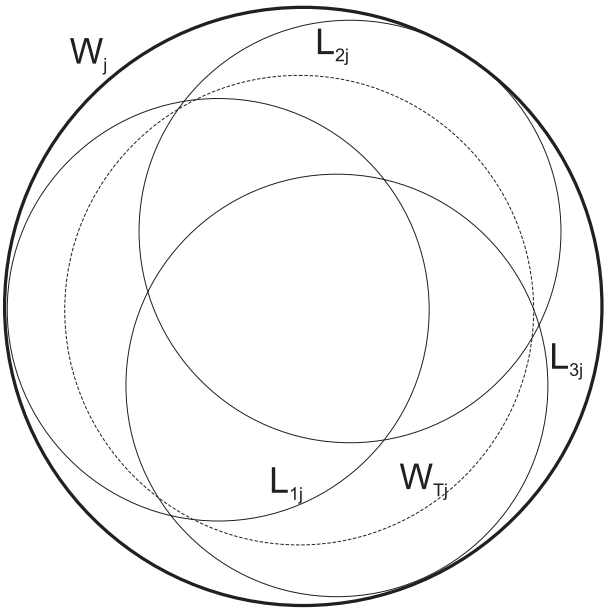

Fig. 3. Relative positions and overlaps of the $N+2$ circular regions. Note that central obstruction is not considered here. As previously, $N=3$ in the drawing.

median conditions the displacement of the footprint is more than one order of magnitude smaller than the Fried parameter. This estimation is even far too pessimistic. In fact it is known that the Fried parameter associated with the higher layers is substantially larger than the overall one (see for instance Roggemann et al., 1995). Hence, the effects of such uncertainty are very small. Furthermore, it is to be pointed out that this phenomenon should affect equally the TF90 technique.

In the following we use the Zernike definition as in Noll (1976). Because it is not accessible, we omit the piston term in the Zernike wavefront expansion. Because of the tip-tilt indetermination problem, we also omit the tip-tilt terms.

Because of this, the demonstration given in Sect. 2 does not strictly apply and one should carry out the following calculations including all the Zernike polynomials and ignoring the first three at the end. In practice one omit these from the beginning and allows for undetermined differences in the piston and tip–tilt terms between the various wavefront involved.

For the i–th LGS, the wavefront can be expanded into a sum of P Zernike polynomials, as:

$$L_i = \begin{bmatrix} a_4 \\ a_5 \\ \vdots \\ a_{P+3} \end{bmatrix} \tag{9}$$

We call L_i the modal expansion (vector of Zernike coefficients) of the wavefront coming from LGS i, integrated over the layers. L_{ij} is the expansion of the wavefront included in the beam coming from LGS i at layer j (footprint of LGS i on layer j). It is clear that the physical dimension of the wavefronts corresponding to the various L_{ij} varies with the layer height. However, we have:

$$L_i = \sum_{j=1}^{M} L_{ij} \tag{10}$$

In a similar way, we can define the expansion of the metapupil, W_j, and the expansion of the science object beam W_{Tj}.

Given the known geometry between these circular regions, one can define a set of matrices A_{ij} of size $P \times P$ such that:

$$L_{ij} = A_{ij}\, W_j \tag{11}$$

It is worth noting that Eq. (11) is an exact relationship, W_j being defined on a region larger and including any of the sub–regions L_{ij}.

The wavefront seen by the i–th wavefront sensor can be expressed as the sum of all the perturbations introduced by all of the M perturbing layers. Putting Eqs. 10 and 11 together leads to:

$$L_i = \sum_{j=1}^{M} L_{ij} = \sum_{j=1}^{M} A_{ij}\, W_j \tag{12}$$

These equations, for all LGSs, can be combined in a single matrix equation, including all the M layers and all the N LGSs in the same relationship:

$$\begin{bmatrix} L_1 \\ L_2 \\ \vdots \\ L_N \end{bmatrix} = \begin{bmatrix} A_{11} & A_{12} & \cdots & A_{1M} \\ A_{21} & A_{22} & \cdots & A_{2M} \\ \vdots & & \ddots & \vdots \\ A_{N1} & A_{N2} & \cdots & A_{NM} \end{bmatrix} \begin{bmatrix} W_1 \\ W_2 \\ \vdots \\ W_M \end{bmatrix} \tag{13}$$

which can be written in a more compact form as:

$$L = A\, W \tag{14}$$

In the same fashion, the wavefront expansion W_j from the metapupil can be projected onto the smaller and co–axial sub–region defined by the projection of the telescope pupil on the j–th layer denoted by the Zernike expansion W_{Tj}:

$$W_{Tj} = T_j\, W_j \tag{15}$$

that defines univoquely the T_j matrix, again of size $P \times P$.

The wavefront perturbation, free from focal anisoplanatism, experienced by the science target on the axis of the telescope, expanded in a Zernike series W_T can now be written as the sum of all the perturbations introduced by all of the M layers and re–written using Eq. (15):

$$W_T = \sum_{j=1}^{M} W_{Tj} = \sum_{j=1}^{M} T_j\, W_j = [T_1\, T_2\, \ldots T_M] \begin{bmatrix} W_1 \\ W_2 \\ \vdots \\ W_M \end{bmatrix} \tag{16}$$

and in a more compact form:

$$W_T = T\, W \tag{17}$$

The matrices A ($N \times P$ rows and $M \times P$ columns) and T (P rows and $M \times P$ columns) are a collection of numerical coefficients rigorously derived from the geometry of the problem. The vector L (including $N \times P$ elements) is estimated by the LGSs fed wavefront sensors. Provided $N \geq M$ (this requires to fire at least as much LGSs as significant layers are in the optical path), using Eqs. (14) and (17) one can easily retrieve W_T that is the desired perturbation of the science target, to be applied to a conveniently placed deformable mirror in order to compensate the atmospheric image degradation. This involves non–square matrices and a least–squares determination must be adopted. This can be done through the use of the *pseudo–inverse* of the generic rectangular matrix X, usually denoted by X^+ (Luenberger, 1969; Wild, 1997; Wild, Kibblewhite & Scor, 1994). Such pseudo–inverse (sometimes reffered as Moore–Penrose inverse) is, under the circumstances we described, unique and is equivalent to the best least–square estimator in an Euclidean space. For instance one can write W_T in terms of A, T and L as both:

$$W_T = T\ A^+\ L = \left(A\ T^+\right)^+\ L \tag{18}$$

While from the analytical point of view, both the derivations are correct we wish to point out that T defines Zernike projections between concentric circular pupils characterized by different diameters, while A includes further some decentering between the relating pupils. For this reason one can expect that T (and hence AT^+) is probably *easier* to invert than A, in terms of better noise rejection.

4. Conclusion

Modal tomography is just a different way to write down the concept of 3D tomographic reconstruction. The resulting formulation is very simple while the derivation is an exact derivation of geometrical properties of the beams involved. The modal approach should leads to an easier implementation, an easier filtering (and hence a more robust rejection of noise) and, in the opinion of the authors, it should be easier to deal with a number of practical situation (e.g. non–zero obstruction of the telescope). A detailed analysis of the technique requires at least an in–deep simulation and is beyond the limits of this Letter. Its extension to deal with the absolute tip–tilt indetermination problem (Ragazzoni & Rigaut, 1998), conical anisokinetism (Esposito, Riccardi & Ragazzoni, 1996; Neymann, 1996) and eventually to include piston term to deal with interferometry with other telescopes can also find space in a through study of the technique.

Acknowledgements. Special thanks are due to Silene Soci for helpful hints in some mathematical treatment and to an anonymous Referee whose suggestions greatly improved the content of this Letter. Thanks are due for the several discussions on related topics to the 8m Laser Guide Star European Training and Mobility Resources Network of the European Community.

References

Esposito S., Riccardi A., Ragazzoni R., 1996, JOSA A 13, 1916
Foy R., Labeyrie A., 1985, A&A 152, L29
Fried D.L., Belsher J.F., 1994, JOSA A, 11, 277
Fried D.L., 1995, JOSA A, 12, 939
Happer W., MacDonald G.J., Max C.E., Dyson F.J., 1994, JOSA A, 11, 263
Luenberger D.G., 1969 "Optimization by Vector Space Methods", John Wiley & Sons ed., New York
Neymann C.R., 1996, Opt.Lett. 21, 1806
Noll R.J., 1976 JOSA 66, 207
Parenti R.R, Sasiela R.J., 1994, JOSA A, 11, 288
Ragazzoni R., Esposito S., Riccardi A., 1998 A&AS 128, 617
Ragazzoni R., Rigaut F., 1998, A&A 338, L100
Roggemann M.C., Welsh B.M., Montera D., Rhoadarmer T.A., 1995, AO 34, 4037
Sasiela R.J., 1994, JOSA A, 11, 379
Tallon, M., Foy, R., 1990, A&A 235, 549 (TF90)
Wild W.J., 1997, SPIE proc. 3126, 278
Wild W.J., Kibblewhite E., Scor V., 1994, SPIE proc. 2201, 726